

Mechanical Analysis of the Uterosacral Ligament: Swine vs. Human

ADWOA BAAH-DWOMOH,¹ MARIANNA ALPERIN,² MARK COOK,³ and RAFFAELLA DE VITA¹

¹STRETCH Laboratory, Department of Biomedical Engineering and Mechanics, Virginia Tech, 330 A Kelly Hall, 325 Stanger Street, Blacksburg, VA 24061, USA; ²Division of Urogynecology and Reconstructive Pelvic Surgery, University of California, San Diego, La Jolla, CA 92093, USA; and ³Department of Integrative Biology and Physiology, University of Minnesota, Minneapolis, MN 55455, USA

(Received 23 January 2018; accepted 19 July 2018)

Associate Editor Elena S. Di Martino oversaw the review of this article.

Abstract—The uterosacral ligament (USL) is a major suspensory structure of the female pelvic floor, providing support to the cervix and/or upper vagina. It plays a pivotal role in surgical procedures for pelvic organ prolapse (POP) aimed at restoring apical support. Despite its important mechanical function, little is known about the mechanical properties of the USL due to the constraints associated with *in vivo* testing of human USL and the lack of validated large animal models that enable such investigations. In this study, we provide the first comparison of the mechanical properties of swine and human USLs. Preconditioning and pre-creep data up to a 2 N load and creep data under a 2 N load over 1200 s were obtained on swine ($n = 9$) and human ($n = 9$) USL specimens by performing planar equi-biaxial tensile tests and using the digital image correlation method. No differences in the peak strain during preconditioning tests, secant modulus of the pre-creep response, and strain at the end of creep tests were detected in the USLs from the two species along both axial loading directions (the main *in vivo* loading direction and the direction that is perpendicular to it). These findings suggest that the swine holds promise as large animal model for studying the mechanical role of the USL in apical vaginal support and treatment of POP.

Keywords—Uterosacral ligament, Elasticity, Viscoelasticity, Biaxial testing, Digital image correlation.

INTRODUCTION

Pelvic organ prolapse (POP) is a very common disorder, affecting up to 50% of women.⁵ The number of women with POP is expected to increase by 46% by 2050 due to the growing older population.⁵¹ This condition, characterized by an abnormal descent of the female pelvic organs, adversely affects women's quality

of life, including social, psychological, occupational, physical, and sexual well-being.^{28,35} Although the etiology has not been fully elucidated, vaginal delivery, obesity, and aging have long been linked to the development of POP. Treatments may vary based upon patient symptoms and preferences but, in many cases, patients opt for surgery. Unfortunately, the success rate of current POP surgeries is low, with 40% of women still experiencing prolapse symptoms 2 years after the surgery.⁶

The goal of pelvic reconstructive surgeries is to restore the pelvic floor support so that the patient can maintain a normal quality of life. For many years, surgeons have used endogenous tissues in these procedures. The most used endogenous structure for apical prolapse repair is the uterosacral ligament (USL). The USL connects the cervix or vagina to the sacrum, providing support to the uterus/cervix/vagina complex. The name “uterosacral ligament” is a misnomer since this is not a ligament in a traditional sense. It is primarily composed of collagen fibers and smooth muscle cells with an autonomic nerve supply and a network of blood vessels.⁴⁰

Given the high failure rate of native tissue POP repairs, surgeons started to augment vaginal POP reconstructions with synthetic mesh grafts. Unfortunately, these grafts are associated with an unacceptable rate of complications,¹⁸ culminating with Public Health Notifications issued by the U.S. Food & Drug Administration. To date, the potential benefits of synthetic meshes in POP repair are unclear. Because of the very important role played by the USL in the normal support of the pelvic organs and in reconstructive surgeries, research is needed to advance our limited knowledge about the mechanical properties of the USL. Indeed, the success of USL suspension

Address correspondence to Raffaella De Vita, STRETCH Laboratory, Department of Biomedical Engineering and Mechanics, Virginia Tech, 330 A Kelly Hall, 325 Stanger Street, Blacksburg, VA 24061, USA. Electronic mail: devita@vt.edu

surgeries relies heavily on the mechanical properties of this ligament and ideal grafts must target the mechanical properties of the endogenous host tissues.

The mechanical behavior of the USL is determined by its composition. Several histological studies have been conducted to identify the main components of the human USL using either tissue from cadavers^{10,15} or from patients undergoing hysterectomy.^{8,9,22,23} Recently, two histological studies have been carried out on USL tissue from other species in order to establish the use of animal models for USL research.^{24,26} Gruber *et al.*²⁴ found that the swine USL contained a moderate amount of collagen, an extensive amount of elastin, and smooth muscle and initially proposed the swine as a possible animal model for POP. Iwanaga *et al.*²⁶ undertook a comparative histological study of human, rat, and mouse USLs and found that the human and rat USLs have comparable collagen and smooth muscle contents, suggesting that the rat is also an appropriate and cost effective animal model. The composition of the USL alone does not necessarily ensure that the mechanical function of the human USL and of the USLs from other species are comparable but mechanical tests are needed. To date, there are no mechanical studies that directly compare the human USL to the USLs from other species.

Ex vivo uniaxial tests have been conducted to characterize the mechanical behavior of the human USL.^{13,37,41,42} In these studies, mechanical data were collected either using cadaveric tissue or fresh tissue collected from women undergoing hysterectomy. The measured mechanical properties were thus inevitably affected by the medical history, age, and parity of the donor/patient. While *ex vivo* studies have provided very valuable information with regards to the elastic and viscoelastic properties of the USL, *in vivo* mechanical tests of the USL, whenever possible, are ideal.^{36,43} However, these tests can be conducted in humans only over a very short period of time due to ethical concerns associated with subjecting patients to mechanical testing for extended periods of time.

The use of large animal models for studying the mechanical function of the USL for the prevention and treatment of POP is crucial since the health state, age, and parity of the animals can be controlled. Using the monkey, Vardy *et al.*⁴⁷ measured the uniaxial elastic and stress relaxation response of USLs while, more recently, we characterized the elastic, stress relaxation and creep properties of the USL (and cardinal ligament) using the swine as animal model.^{1,2,7,45,46} In addition to uniaxial tensile tests,⁴⁶ planar biaxial tensile tests, which better emulate the complex *in vivo* loading conditions of the USL, were performed.^{2,7,45}

This study presents a direct comparison of the mechanical properties of swine and human USLs in

order to evaluate the swine as an animal model for POP. Unlike previous studies, the preconditioning/cyclic loading, pre-creep/elastic, and creep responses of USL specimens under biaxial loading are determined by performing detailed and accurate strain analysis using the digital image correlation method (DIC). To our knowledge, there are no published studies that directly compare the biaxial mechanical properties of human USL to those of USL from other species. Additionally, there are no studies that present biaxial mechanical data of human USL tissue. The findings of this novel research will not only provide a preliminary evaluation of the swine as large animal model for mechanical testing of the USL but also offer new mechanical data on human USL.

MATERIALS AND METHODS

Swine Specimen Preparation

This study was conducted with the approval of the Institutional Animal Care and Use Committee (IACUC) at Virginia Tech. Eleven adult (3–4 year-old, approximately 450 lbs) domestic swine were obtained from a slaughterhouse (Gunnore Sausage Co., Goode, VA). Nine swine were used for mechanical testing and two for histology. The USLs were harvested from the swine using previously detailed techniques⁴⁶ in the region extending from the cervix to and around the rectum. Given the size of the USL, only one square specimen was selected from each swine for mechanical testing. The specimens ($n = 9$) were hydrated in phosphate-buffered saline solution (PBS, pH 7.4, Fisher Scientific, USA) and stored at -20°C until testing. For histological analysis, $n = 4$ specimens (2 from each swine) were harvested from the USLs and immediately placed in 10% buffered formalin solution.

Human Specimen Preparation

Human fresh cadaveric bilateral USLs were procured from four unpreserved female donors, whose medical records were available for review, through collaboration with the Bequest Body Donation Program at the University of Minnesota. Donors with history of symptomatic POP, pelvic reconstructive surgeries, hysterectomy, pelvic malignancy, pelvic radiation, connective tissue disorders, myopathy, or POP distal to the hymen on post-mortem examination facilitated by the Credé's Maneuver were excluded. The study was exempt from the Institutional Review Board approval, as it did not include living human subjects. The average age and body mass index of the cadaveric donors were 65.5 ± 12.3 years (mean \pm

standard deviation (SD)) and $23.2 \pm 5.5 \text{ kg/m}^2$ (mean \pm SD), respectively. Out of four donors, three were nulliparous and one was parous, with history of three vaginal deliveries. Bilateral USLs were identified by tracking each ligament along its length from origin to insertion and harvested in their entirety within 96 h post-mortem. The proximal ends of the ligaments were tagged with a single suture to guide specimen orientation during subsequent mechanical testing. The USLs were stored in PBS solution at 4 °C and shipped overnight on ice to Virginia Tech.

Once received, due to size limitations, seven USL square specimens were isolated from seven of the eight USLs and two USL square specimens were isolated from one USL for mechanical testing. These specimens ($n = 9$) were stored in PBS at -20°C until mechanical testing. Specimens intended for histological analysis ($n = 4$) were collected from the remaining portions of the USL that included the mid to distal regions ($n = 2$) and mid to proximal regions ($n = 2$). They were placed in 10% buffered formalin and stored in 70% ethanol until testing at room temperature.

Histology

Swine and human USL specimens were gradually dehydrated in a graded ethanol and xylol series, embedded in paraffin wax, and cut into $4 \mu\text{m}$ thin sections with a microtome. Four sections from each specimen were stained with the Masson's trichrome (MT) and four sections with the Verhoeff–van Gieson (VVG). The histological slides were examined under a light microscope (DMI6000B, Leica Microsystems, Bannockburn, IL, USA) equipped with a scanning stage (LMT260, Leica Microsystems, Bannockburn, IL, USA) at $\times 40$ magnification and images were collected using a digital microscope camera (DMC4500, Leica Microsystems, Bannockburn, IL, USA). Smooth muscle and collagen contents were determined from the MT-stained slides while elastin content was quantified from the VVG-stained slides. Five areas ($1160 \times 870 \mu\text{m}^2$) were randomly selected per each cross-section and divided into 4×4 tiles ($290 \times 218 \mu\text{m}^2$) for quantification analysis with a color deconvolution plug-in (<http://4n6site.com>) of Adobe Photoshop software and ImageJ (NIH, MD), using previously published protocols.^{26,33} Briefly, the color representing one component (e.g., blue for collagen using the MT method) was selected while all other colors were eliminated from the image using Adobe Photoshop software. Then, using ImageJ, the number of pixel that remained in that color were counted and divided by the total number of colored

pixels (excluding white pixels) in the entire image. This number represented the relative content of that component. It was averaged over the five random areas selected from a given histological slide and over the total number of slides ($n = 4$ swine USLs or $n = 4$ human USLs).

Mechanical Testing

The ligaments were thawed at room temperature and cut into squares ranging from approximately $2.3 \times 2.3 \text{ cm}^2$ to $3 \times 3 \text{ cm}^2$ specimens. The thickness of each specimen was measured in 4 different locations using a digital caliper (accuracy: $\pm 0.05 \text{ mm}$, Series 573, Mitutoyo, Japan) under a 50 g compressive load and the average was computed. The specimen was gripped with 4 safety pins on each of the four sides and mounted into an Instron planar biaxial testing system equipped with four 20 N load cells (accuracy: $\pm 0.02 \text{ N}$, Instron, UK). The two axial loading directions were selected in the main *in vivo* loading direction of the USL and the direction perpendicular to it. For each specimen, the distances between the safety pins were used to compute the side length of the specimens using ImageJ (NIH, Bethesda, MD). These lengths were then multiplied by the specimen's average thickness to determine the specimen's undeformed cross-sectional area along the main *in vivo* and perpendicular loading directions. The specimen was then lowered into a bath made of acrylic glass (Perspex, UK) which was filled with PBS at room temperature (21°C). A cover, also made of acrylic glass, was placed over the bath, making complete contact with the PBS to avoid subtle fluid movements that could influence the strain measurement.

The 3D DIC technique was employed for non-contact strain measurement. The DIC system (VIC-3D, Correlated Solutions, Columbia, SC) consisted of two CCD cameras (Prosilica GX 1660, Allied Vision Technologies, Exton, Pennsylvania, USA) equipped with macro lenses (AT-X 100 mm F2.8 AT-X M100 Pro D Macro Lens, Tokina, Tokyo, Japan) that were utilized to capture high resolution (1600×1200 pixels) images of each specimen during testing. Before each test, images of a $12 \times 9 \text{ mm}^2$ plastic grid with 4 mm spacing were taken in order to calibrate the system. Each specimen was immersed in a solution of PBS and methylene blue, 1% aqueous solution (Fisher Science Education, USA) and a speckle pattern was created on the surface of the specimen using an aerosol fast dry gloss white paint (McMaster-Carr, USA).³⁴

Both swine specimens ($n = 9$) and human specimens ($n = 9$) were preloaded to 0.1 N and preconditioned

by loading/unloading them from 0.1 to 2 N ten times at 0.05 N/s loading rate in both axial loading directions. Following preconditioning, the specimens were unloaded and allowed to recover for 600 s (= 10 min). They were then stretched along the two loading directions at 0.05 N/s loading rate until an equi-biaxial load of 2 N was reached. The equi-biaxial load of 2 N was held constant for 1200 s (= 20 min). The load level was selected based on previous studies conducted by Luo *et al.*³⁶ The time interval for creep tests was chosen based on the work by Tan *et al.*⁴⁵ showing that the largest increase in strain for the swine USL/cardinal ligament complex occurred over the first 20 min.

For each specimen, preconditioning/cyclic, pre-creep/elastic, and creep data were collected in the main *in vivo* loading direction and in the perpendicular direction. For the preconditioning/cyclic, pre-creep/elastic, and creep portions of the test, the nominal normal stress in the main *in vivo* or perpendicular loading direction for each specimen was calculated by dividing the axial load in that direction by the specimen's undeformed cross sectional area that was perpendicular to such direction. This quantity will be referred simply as "stress" hereafter. Using the DIC method, the Lagrangian strain of each tested specimen was calculated. More specifically, a square region was selected in the center of each specimen and the local normal Lagrangian strain in both axial loading directions at every second for the entire duration of each test (preconditioning/cyclic, pre-creep/elastic, and creep tests) was recorded. These local normal Lagrangian strains were then averaged over this square region, resulting, at every second, in a single average normal Lagrangian strain value along the main *in vivo* loading direction and a single average normal Lagrangian strain value along the perpendicular loading direction for a given specimen. The average normal Lagrangian strain calculated for one specimen in each of the axial loading directions will be further referred simply as "strain" in such direction.

The secant modulus for each specimen in each loading direction was computed as the slope of a secant line drawn from the first and last point of the pre-creep/elastic stress-strain curve in such direction. In each loading direction, the strain during creep was also normalized by dividing it, at each second, by the corresponding pre-creep peak strain. Moreover, the creep rate in the main *in vivo* or perpendicular loading direction was calculated for each specimen as the slope of the linear regression line of the normalized strain vs. time data in the corresponding direction using logarithmic scales.²⁵

Statistical Analysis

The Student's *t* test was used to compare the mean relative content of a given component in swine and human USLs ($\alpha = 0.05$) and the mean peak strain during preconditioning and creep for human or swine USLs in each loading direction. An analysis of variance followed by Fishers LSD *post hoc* analysis ($\alpha = 0.05$) was used to compare the mean peak strains recorded during preconditioning, the mean secant moduli of the pre-creep stress-strain curve, mean of the minimum, average (over the square region selected for strain measurement), and maximum strains at the end of the creep test ($t = 1200$ s), and the mean creep rates across directions (main *in vivo* and perpendicular directions) and species (swine and human). All data are presented as mean \pm standard error of the mean (SEM), unless noted otherwise. All statistical analyses were conducted using Minitab statistical software (Minitab 17, Minitab Inc.).

RESULTS

Both swine and human USLs are composed predominantly of collagen, followed by smooth muscle, with elastin representing the least abundant component. Figure 1 shows representative images of swine and human USLs stained with MT and VVG with collagen bundles, smooth muscle fibers, elastin, nerve fibers, arteries, and veins clearly visible in both groups. No significant differences were found in relative collagen content (swine: $83.31 \pm 2.13\%$ vs. human: $78.32 \pm 1.97\%$, $p > 0.05$) and in relative smooth muscle content (swine: $16.69 \pm 2.13\%$ vs. human: $21.67 \pm 1.97\%$ for human, $p > 0.05$) between species. In contrast, the relative elastin content of swine USL was significantly lower than that of the human USL (swine: $5.91 \pm 0.69\%$ vs. human: $7.01 \pm 0.87\%$, $p < 0.05$).

Both swine and human USL specimens experienced lower strains in the main *in vivo* loading direction compared to the perpendicular loading direction during preconditioning (Fig. 2a). However, when comparing the mean peak strains during preconditioning across loading directions and species, no significant differences were found ($p > 0.05$) (Fig. 2b).

The mean stress-strain data computed from both swine and human USL specimens during the pre-creep tests are reported in Fig. 3a. From the mean stress-strain curves, the human USL appeared to be stiffer than the swine USL. The mean secant moduli of the

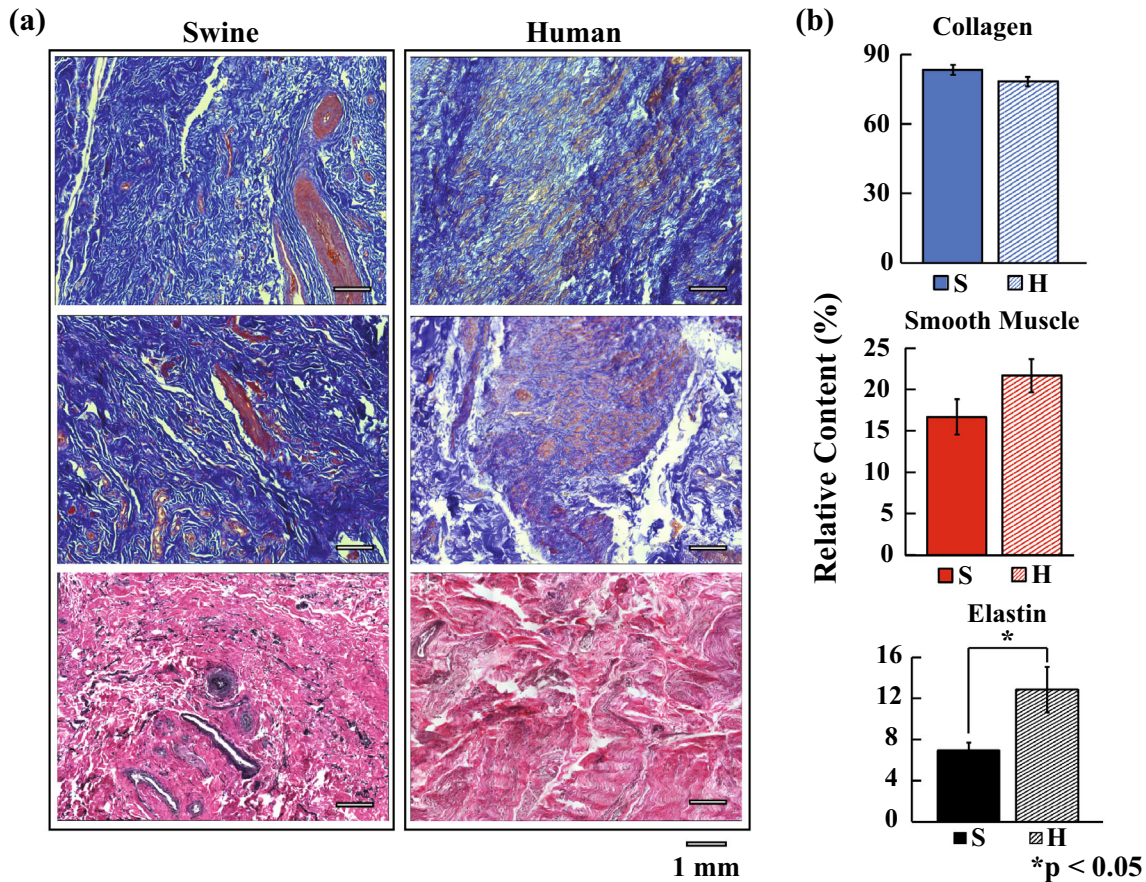


FIGURE 1. (a) Swine and human USL histological slides with MT stain and VVG stain. (b) Relative collagen, smooth muscle, and elastin contents of swine and human USLs.

stress-strain curves are reported in Fig. 3b. For human USL specimens, the mean secant moduli in the main *in vivo* and perpendicular loading directions were 7.76 ± 1.65 and 6.00 ± 1.35 MPa, respectively. For swine USL specimens, the mean secant moduli in the main *in vivo* and perpendicular loading directions were 3.51 ± 0.61 and 4.87 ± 1.94 MPa, respectively. No significant differences were found when comparing the secant moduli of the stress-strain curves across loading directions and species ($p > 0.05$).

The mean stresses for human USL specimens ($n = 9$) subjected to creep tests at 2 N equi-biaxial load were found to be 0.16 and 0.17 MPa in the main *in vivo* and perpendicular loading directions, respectively (Table 1). The mean stresses for swine USL specimens ($n = 9$) subjected to creep tests at 2 N equi-biaxial load were found to be 0.10 and 0.09 MPa in the main *in vivo* and perpendicular loading directions, respectively (Table 1). The mean initial creep strain (i.e. the mean strain at the beginning of creep at $t = 0$) was lower, but not significantly lower, in the main *in vivo* loading direction compared to the perpendicular loading direction for both swine and human USL specimens.

No significant differences were found when comparing the mean initial creep strains across loading directions and species ($p > 0.05$).

During creep, the mean strain over time always remained lower in the main *in vivo* loading direction compared to the perpendicular loading direction for both swine and human USL specimens (Fig. 4). However, at the end of the creep test ($t = 1200$ s), the minimum, average, and maximum strains for both swine and human USL specimens along both loading directions were compared (Fig. 5). No significant differences were found for both swine and human USL specimens along both loading directions ($p > 0.05$).

The mean normalized strain vs. time data obtained during creep tests and the corresponding creep rates are shown in Fig. 6. For human USL specimens, the mean peak strain during creep (or equivalently, the mean strain at the end of creep) was found to be 1.09 and 1.15 times the mean initial creep strain in the main *in vivo* and perpendicular loading directions, respectively. For swine USL specimens, the mean peak strain during creep was found to be 1.12 and 1.16 times the mean initial creep strain in the main *in vivo* and

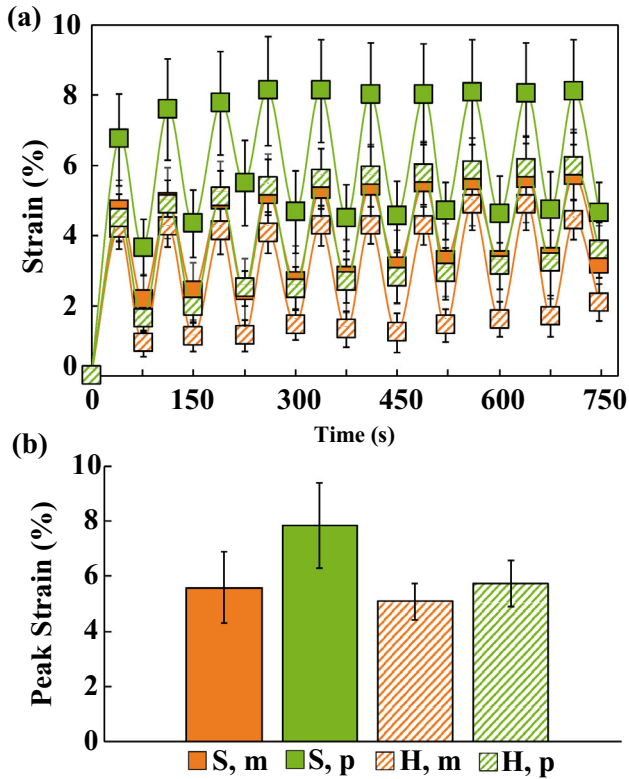


FIGURE 2. (a) Mean (\pm SEM) strain vs. time and (b) mean peak strain in the main *in vivo* and perpendicular loading directions of human USL specimens ($n = 9$) and swine USL ($n = 9$) specimens subjected to ten preconditioning cycles from 0.1 to 2 N equi-biaxial loads (S denotes data from swine USL, H data from human USL, m data in the main *in vivo* loading direction, and p data in the perpendicular loading direction).

perpendicular loading directions, respectively. For both swine and human specimens, the mean normalized strain over time was larger in the perpendicular loading direction compared to the main *in vivo* loading direction. For human USL specimens, the mean creep rate was 0.020 ± 0.003 and 0.028 ± 0.006 1/s in the main *in vivo* and perpendicular loading directions, respectively, and, for swine USL specimens, it was 0.029 ± 0.008 and 0.031 ± 0.008 1/s in the main *in vivo* and perpendicular loading directions, respectively. No significant differences were found when comparing the mean creep rates across loading directions and species ($p > 0.05$).

In Fig. 7, the comparison of the mean peak strain computed during preconditioning with the mean peak strain computed during creep, that is at the end of the creep test, for swine and human USL specimens for each loading direction is shown. Both swine and human USL specimens showed higher mean peak strain during preconditioning than during creep for both loading directions ($p < 0.05$ for the preconditioning vs. creep comparison for human USL specimens in

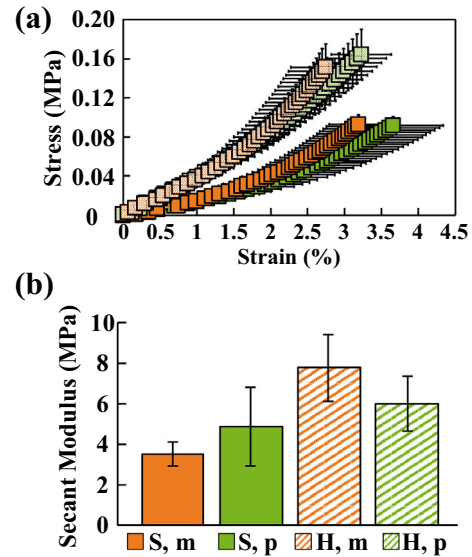


FIGURE 3. Mean (\pm SEM) of (a) pre-creep stress-strain curves and (b) secant moduli of the pre-creep stress-strain curves in the main *in vivo* and perpendicular loading directions for swine USL specimens ($n = 9$) and human USL specimens ($n = 9$) equi-biaxially loaded up to 2 N (S denotes data from swine USL, H data from human USL, m data in the main *in vivo* loading direction, and p data in the perpendicular loading direction).

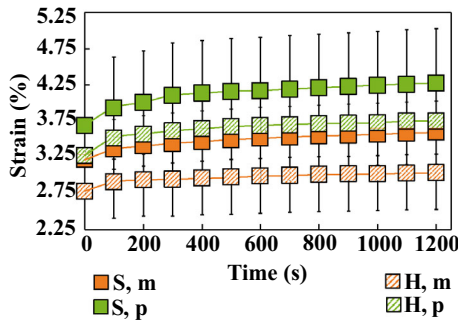
the main *in vivo* loading direction, $p > 0.05$ for all other comparisons).

DISCUSSION

This study compared the mechanical behavior of the swine and human USLs. Under cyclic equi-biaxial loads to 2 N, during preconditioning, the swine USL appeared to achieve higher mean peak strains (5.70% and 8.12% in the main *in vivo* and perpendicular loading directions, respectively) than human USL (4.90% and 5.98% in the main *in vivo* and the perpendicular loading directions, respectively) (Fig. 2). However, no statistical differences were found amongst the mean peak strain across species and directions. Similarly, no statistical differences were found in the mean secant modulus of the pre-creep stress-strain curve across species and directions although the mean secant modulus was higher for the human USL (Fig. 3). During equi-biaxial creep tests at 2 N, the swine USL achieved higher mean strain (and normalized strain) over time in each loading direction than the human USL but, again, no statistical differences were found when comparing the mean peak strain during creep and the mean creep rates across species and loading directions (Figs. 4, 5, and 6). Overall the swine USL was found to be mechanically similar to the human USL, suggesting that the swine is

TABLE 1. Creep test parameters for human USL specimens with mean (\pm SD) thickness of 0.78 ± 0.33 mm ($n = 9$) and swine USL specimens with mean (\pm SD) thickness of 0.92 ± 0.29 mm ($n = 9$).

Species	Mechanical quantity	Loading direction	Value (mean \pm SEM)
Human	Stress (MPa)	Main <i>in-vivo</i>	0.16 ± 0.02
		Perpendicular	0.17 ± 0.03
	Initial creep strain (%)	Main <i>in-vivo</i>	2.78 ± 0.47
		Perpendicular	3.27 ± 0.41
Swine	Stress (MPa)	Main <i>in-vivo</i>	0.10 ± 0.01
		Perpendicular	0.09 ± 0.01
	Initial creep strain (%)	Main <i>in-vivo</i>	3.21 ± 0.40
		Perpendicular	3.69 ± 0.76

**FIGURE 4. Mean (\pm SEM) strain vs. time for human USL specimens ($n = 9$) and swine USL ($n = 9$) specimens in the main *in vivo* and perpendicular loading directions subjected to 2 N equi-biaxial load (S denotes data from swine USL, H data from human USL, m data in the main *in vivo* loading direction, and p data in the perpendicular loading direction).**

a good large animal model for testing the mechanical properties of the USL.

Our quantitative analysis of MT-stained and VVG-stained histological sections indicated that swine and human USLs had comparable relative collagen and smooth muscle content but different elastin content (Fig. 1). Several studies have been conducted to identify the main components of the USL but only a few have quantified their contents in human or swine USLs.^{22,24,26} Gabriel *et al.*²² analyzed the composition of the cervical portion of the USLs in postmenopausal women *via* immunohistochemistry techniques and found that the USL from women without prolapse exhibited approximately 25% smooth muscle content.²² These results are comparable to the results obtained in our study for human USL despite the fact that the histological sections of the human USL were isolated from different regions. The first histological study on the USL from swine was published by Gruber *et al.*²⁴ These authors described the collagen and elastin content with a subjective 1- to 5-point scale, where 1 indicated no collagen or elastin content and 5 indicating extensive collagen or elastin content. The collagen content was rated 2.5 and the elastin content was

rated 5 for the USL in comparison to the elastin content of the vagina and cardinal ligament. Given the large amount of elastin reported by Gruber *et al.*,²⁴ we also employed the VVG staining method to detect the relative amount of elastin in swine and human USLs. Our analysis showed that the swine USL had a significantly lower elastin content than human USL. In general, elastin in connective tissues allows for elastic strain recovery and resilience and, specifically in the human USL, large amount of elastin may be needed to allow a wide range of movements of the pelvic organs.^{24,29}

In this study, we preconditioned swine and human USL specimens by applying cyclic loading at a constant magnitude and loading rate. Preconditioning reduces residual stresses in soft tissues and provides a repeatable no-load reference configuration.²¹ The strain was found to increase slightly over time and reached a steady state after ten cycles (Fig. 2). In early studies by Fung on mesenteric membranes,^{19,20} which are similar to the USLs,⁴⁰ the loading and unloading curves which were obtained by cyclically loading the membranes at a constant amplitude and elongation rate, never reached a steady state, even after several cycles. However, the difference in load recorded in successive cycles was observed to decrease with the number of cycles as in our study. Over the past years, a variety of preconditioning protocols have been proposed for soft tissues^{11,12,14,39,50} but no consensus has been reached on the ideal protocol. More recently, some investigators have suggested that preconditioning protocols must be selected based on the mechanical tests that are performed. More specifically, a preconditioning protocol that includes both cyclic loading and stress relaxation tests with long recovery periods should be employed for characterizing the stress relaxation response.^{11,12} In our study, the protocol recommended by Carew *et al.*^{11,12} would have been unfeasible. We had to limit the overall testing time since the quality of the speckle pattern created for the DIC strain measurement was compromised with time.

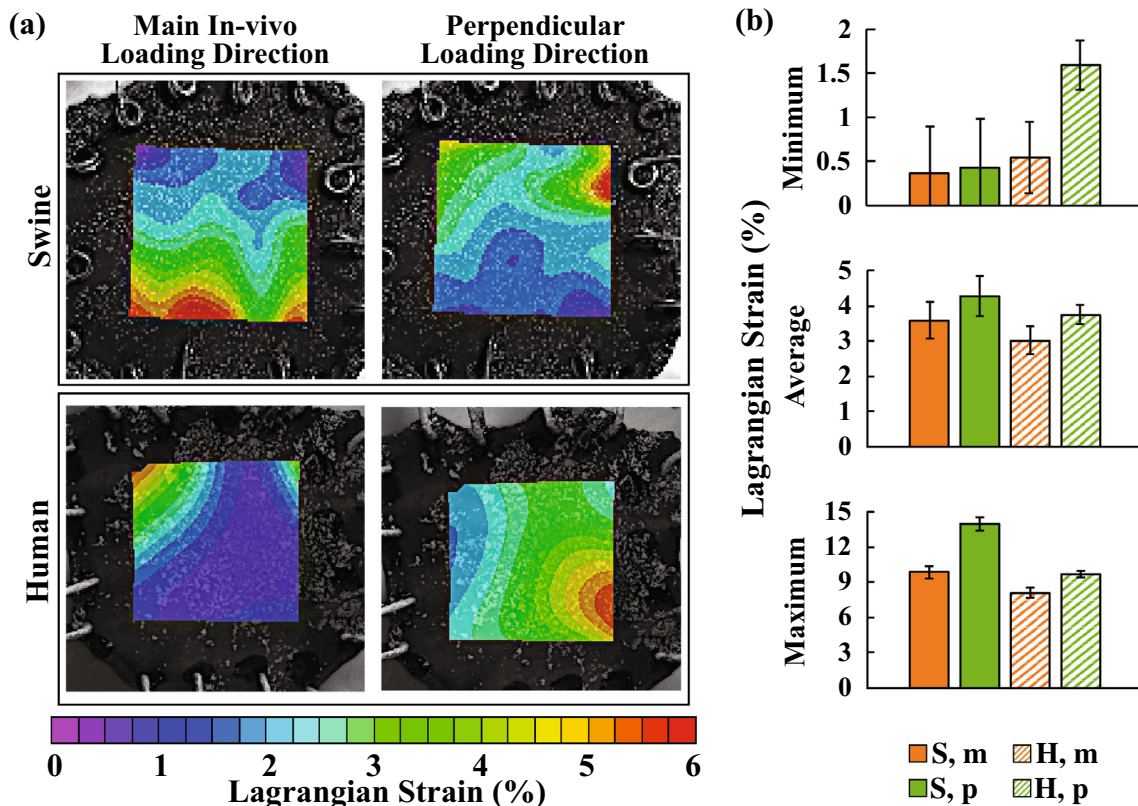


FIGURE 5. (a) Local axial Lagrangian strain map of representative swine and human USL specimens in the main *in vivo* and perpendicular loading directions at the end of creep at $t = 1200$ s. Note that safety pins were used for clamping both swine and human specimens but, for the selected images, the springs are on the top of the swine specimen and on the bottom of the human specimen. (b) Mean (\pm SEM) of the minimum, average, and maximum axial Lagrangian strains in the main *in vivo* and perpendicular loading directions for swine USL specimens ($n = 9$) and human USL specimens ($n = 9$). (S denotes data from swine USL, H data from human USL, m data in the main *in vivo* loading direction, and p data in the perpendicular loading direction).

Overall, swine and human USLs exhibited a comparable elastic and creep response (Figs. 3, 4, 5, and 6). However, the human USL appeared to be slightly stiffer than the swine USL. This was confirmed by the slightly higher mean secant modulus of the stress-strain curve in both loading directions for the human USL when compared to the swine USL (Fig. 3). Moreover, the swine USLs deformed more, but not significantly more, than the human USLs during creep (Figs. 4 and 5). These difference may be attributed, in part, to the differences in how the swine and human tissues were handled post-mortem. Before mechanical testing, the swine USLs were dissected within 4 h of death and then placed in PBS at -20°C while the human USLs were dissected 96 h post-mortem and then preserved in PBS at -20°C . The onset of rigor mortis, which is marked by a shortening of muscle fibers and an increase in the rates of glycolysis, lactic acid levels, and adenosine diphosphate levels in tissues, has been shown to be delayed by a decrease in temperature.^{3,4,30–32,38} The human USL was thus able to achieve higher levels of rigor mortis than the swine

USL. This may have contributed to the increase in stiffness measured during pre-creep tests and decrease in strain measured during creep tests for the human USL.

While no studies report the secant moduli of the USL computed *via* biaxial testing, some studies have reported the elastic modulus of the USL computed from the linear region of the stress-strain curve collected along the main *in vivo* loading direction *via* uniaxial tests.^{37,46,47} In the study by Vardy *et al.*,⁴⁷ elastic moduli of postmenopausal monkey USLs were determined at different strain levels from incremental pre-relaxation stress-strain curves, reaching a value of 1.00 MPa at 30% strain. By testing USLs up to failure, Martins *et al.*³⁷ reported a mean value of 14.1 MPa, ranging from 5.7 to 26.1 MPa, for human USLs while Tan *et al.*⁴⁶ reported values that ranged from 0.5 to 3 MPa for the toe region and from 20 to 39 MPa for the linear region for swine USLs. These values are comparable to the secant moduli that are reported for swine and human USLs in our study (Figure 3). In our study, the stress-strain data were collected during pre-

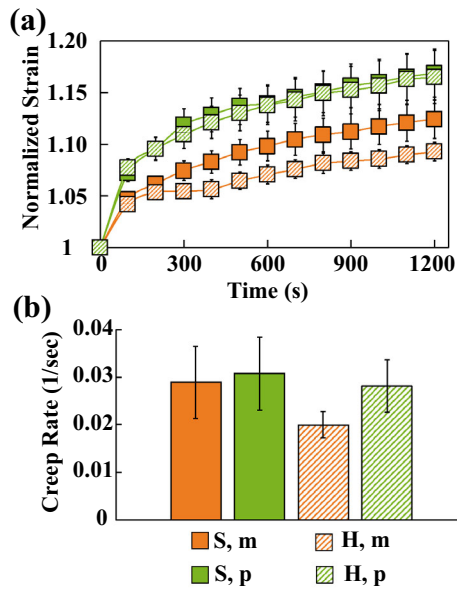


FIGURE 6. Mean (\pm SEM) of (a) normalized strain vs. time and (b) creep rates in the main *in vivo* and perpendicular loading directions during creep at 2 N equi-biaxial load for swine USL specimens ($n = 9$) and human USL specimens ($n = 9$) (S denotes data from swine USL, H data from human USL, m data in the main *in vivo* loading direction, and p data in the perpendicular loading direction).

creep tests by equi-biaxially loading the USL specimens only up to 2 N. Therefore, we obtained lower stresses (Table 1) that those reported in previous studies^{37,46} and, consequently, lower values of the secant moduli.

Obtaining human USLs from healthy fresh cadavers was challenging. The human donors were post-menopausal and their age and parity could not be controlled. Similarly, the swine were of comparable weight but their age and parity were not controlled, and they were not ovariectomized to surgically induce menopause. These differences among swine and human subjects have likely introduced variability in the collected mechanical data. For example, menopause has been shown to alter the mechanical properties of the USLs in monkeys⁴⁷ and women undergoing hysterectomy.⁴¹ Moreover, only nine human specimens were tested and the results were compared to an equal number of swine specimens. We conducted a statistical power analysis with each data set that is presented in this study and determined that the statistical power ranged between 0.28 and 0.35. These values are quite low and approximately 125–135 specimens would be required to detect a possible difference in mechanical properties between human and swine specimens. The lack of a large controlled number of specimens was clearly a limitation of this study as well as a limitation of similar studies. As mentioned previously, there is only one study that compares human USL to USLs

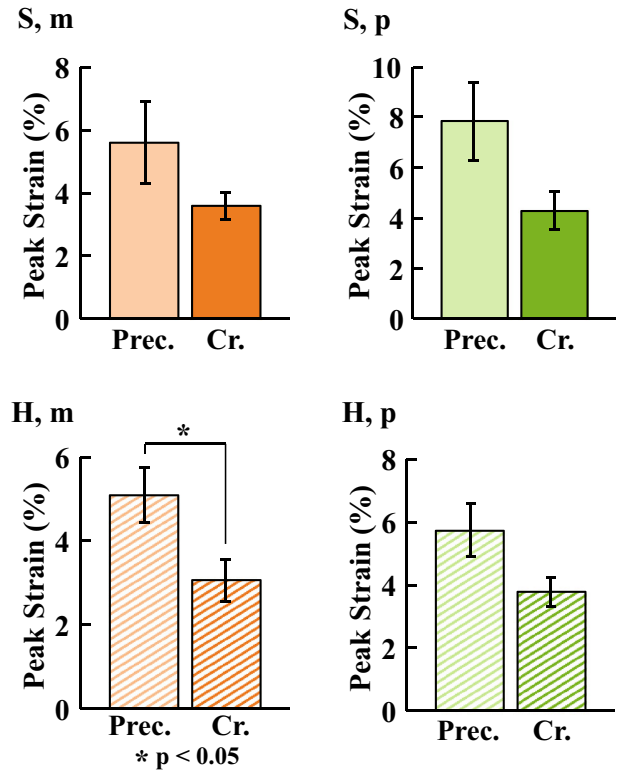


FIGURE 7. Mean (\pm SEM) peak strains calculated during preconditioning and creep (at the end of creep at $t = 1200$ s) in the main *in vivo* and perpendicular loading directions for swine USL specimens ($n = 9$) and human USL specimens ($n = 9$). (S denotes data from swine USL, H data from human USL, m data in the main *in vivo* loading direction, and p data in the perpendicular loading direction).

from other species, and it solely focuses on histology.²⁶ In the cited histological study, only 3–4 specimens from each species were compared.

The DIC method was used throughout the preconditioning/cyclic loading, pre-creep/elastic, and creep tests for non-contact strain measurements. As shown in Fig. 5a, the measured Lagrangian strain was not uniform across the specimens. The differences in strain can be better appreciated by comparing the minimum, maximum, and average strain values reported in Fig. 5b. The non-homogeneous deformation may be the result of inherent inhomogeneities of the specimens but it may be also determined by the clamping technique. Indeed, several studies have shown that clamping techniques affect the strain fields in planar biaxial testing of soft tissues.^{17,27,44,48,49} For nonlinear materials, Eilaghi *et al.*¹⁷ concluded that having the attachment points span a wide zone along each edge of the specimen leads to a more uniform strain field. These investigators also noted that any shifts in the alignment of the attachment points along one edge of the specimen can significantly distort the strain field. Precautions were taken in our study to ensure the

alignment of the pins along each side of the specimens by using a stamp to mark the points where the safety pins were to be inserted and a plastic grid to guide the safety pin placement. However, misalignment of the attachment points was inevitable due to the soft nature of the specimens, and this likely affected the strain field uniformity.

Preconditioning data are rarely published since, as discussed above, preconditioning is only used to establish a repeatable no-load reference configuration. Many investigators in biomechanics have questioned the benefits of preconditioning and they have excluded it from their protocols. We opted to present the mechanical data we collected during preconditioning since, if preconditioning is not deemed necessary, these data can be interpreted as cyclic loading data. We then compared the mean peak strain during preconditioning/cyclic loading to the mean peak strain during creep for both the swine and human USL specimens (Fig. 7). Our goal was to determine differences in strain of the USL under cyclic equi-biaxial loads of 2 N at constant loading rate and under constant equi-biaxial loads of 2 N over time. From our results, strains achieved during cyclic loading were higher than those achieved during creep for both species in both loading directions. Specifically for human tissue, the mean peak strain achieved during cyclic loading was significantly higher than the mean peak strain achieved during creep along the main *in vivo* loading direction (Fig. 7). Even though both cyclic loading and creep tests were performed up to the same load magnitude, USL specimens experienced higher loading rates during cyclic loading than during creep. This explains why higher strains were experienced by the USL specimens during cyclic loading. These findings may suggest that certain exercises, such as exercises where the USL are under constant loads over time (e.g., a squat or a wall sit for a prolonged amount of time) may cause less damage to the pelvic supportive ligaments than exercises where the loads are oscillating at a constant load rate (e.g., a high rep of squats or leg lunges).

Although the etiology of POP is unknown and likely multifactorial, alterations in the mechanical properties of the female pelvic supportive tissues are, without doubt, contributing factors.² Due to limited sample size and ethical concerns with examining human tissue, the selection of appropriate animal models for mechanical testing of pelvic tissues is crucial not only to explore the etiology of POP but also to develop new surgical techniques and better graft materials. Different animal models such as mice, rats, rabbits, sheep, swine, and nonhuman primates have been used to study POP.¹⁶ Through this novel study, we have demonstrated the remarkable mechanical similarities between swine and human USLs. Our results together

with the low cost and ease of breeding of swine and the fact that the swine naturally develops POP suggest that the swine holds promise as an animal model for perturbing the effects of variable conditions on the USL physiological properties.

CONCLUSIONS

Through this comparative mechanical study, we have shown that the swine has the potential to be a good large animal model for testing the mechanical properties of the USL. Swine and human USLs exhibit similar preconditioning/cyclic loading, pre-creep/elastic, and creep properties measured *via* planar biaxial testing in combination with DIC. The findings of this study will hopefully prompt future research on the supportive function of the USL using the swine as animal model to assess novel therapies for POP.

ACKNOWLEDGMENTS

Funding was provided by NSF PECASE Grant No. 1150397 (PI: De Vita) and NIH R03 Grant No. R03AG050951 (PI: Alperin). The authors thank the individuals who donated their bodies to the University of Minnesota's Anatomy Bequest Program for the advancement of education and research.

CONFLICT OF INTEREST

The authors have no conflict of interest.

REFERENCES

- ¹Baah-Dwomoh, A. and R. De Vita. Effects of repeated biaxial loads on the creep properties of cardinal ligaments. *J. Mech. Behav. Biomed.* 74:128–141, 2017.
- ²Baah-Dwomoh, A., J. McGuire, T. Tan, and R. De Vita. Mechanical properties of female reproductive organs and supporting connective tissues: a review of the current state of knowledge. *Appl. Mech. Rev.* 68:060801, 2016.
- ³Bate-Smith, E. and J. Bendall. Factors determining the time course of rigor mortis. *J. Physiol.* 110:47–65, 1949.
- ⁴Bate-Smith, E. and J. Bendall. Changes in muscle after death. *Br. Med. Bull.* 12:230–235, 1956.
- ⁵Barber, M. and C. Maher. Epidemiology and outcome assessment of pelvic organ prolapse. *Int. Urogynecol. J.* 24:1783–90, 2013.
- ⁶Barber, M. D., L. Brubaker, K. L. Burgio, H. E. Richter, I. Nygaard, A. C. Weidner, S. A. Menefee, E. S. Lukacz, P. Norton, J. Schaffer, J. N. Nguyen, D. Borello-France, P. S. Goode, S. Jakus-Waldman, C. Spino, L. K. Warren, M. G. Gantz, and S. F. Meikle. Eunice Kennedy Shriver National Institute of Child Health and Human Development Pelvic

- Floor Disorders Network. Comparison of 2 transvaginal surgical approaches and perioperative behavioral therapy for apical vaginal prolapse: the OPTIMAL randomized trial. *JAMA* 311:1023–1034, 2014.
- ⁷Becker, W. R. and R. De Vita. Biaxial mechanical properties of swine uterosacral and cardinal ligaments. *Bio-mech. Model. Mechanobiol.* 14:549–560, 2015.
- ⁸Butler-Manuel, S. A., L. D. Buttery, R. P. A'Hern, J. M. Polak, and D. P. Barton. Pelvic nerve plexus trauma at radical hysterectomy and simple hysterectomy. *Cancer* 89:834–841, 2000.
- ⁹Butler-Manuel, S. A., L. D. Buttery, J. M. Polak, R. A'Hern, and D. P. Barton. Autonomic nerve trauma at radical hysterectomy: The nerve content and subtypes within the superficial and deep uterosacral ligaments. *Re-prod. Sci.* 15:91–96, 2008.
- ¹⁰Campbell, R. M. The anatomy and histology of the sacrouterine ligaments. *Am. J. Obstet. Gynecol.* 59:1–12, 1950.
- ¹¹Carew, E. O., J. Barber, and I. Vesely. Role of preconditioning and recovery time in repeated testing of aortic valve tissues: validation through quasilinear viscoelastic theory. *Ann. Biomed. Eng.* 28:1093–1100, 2000.
- ¹²Carew, E. O., A. Garg, J. E. Barber, and I. Vesely. Stress relaxation preconditioning of porcine aortic valves. *Ann. Biomed. Eng.* 32:563–572, 2004.
- ¹³Chanterreau, P., M. Brieu, M. Kammal, J. Farthmann, B. Gabriel, and M. Cosson. Mechanical properties of pelvic soft tissue of young women and impact of aging. *Int. Urogynecol. J.* 25:1547–1553, 2014.
- ¹⁴Cheng, S., E. C. Clarke, and L. E. Bilston. The effects of preconditioning strain on measured tissue properties. *J. Biomech.* 42:1360–1362, 2009.
- ¹⁵Cole, E. E., P. B. Leu, A. Gomelsky, P. Revelo, H. Shappell, H. M. Scarpero, and R. R. Dmochowski. Histopathological evaluation of the uterosacral ligament: is this a dependable structure for pelvic reconstruction? *BJU Int.* 97:345–348, 2006.
- ¹⁶Couri, B. M., A. T. Lenis, A. Borazjani, M. F. R. Paraiso, and M. S. Damaser. Animal models of female pelvic organ prolapse: Lessons learned. *Expert. Rev. Obstet. Gynecol.* 7:249–260, 2012.
- ¹⁷Eilaghi, A., J. G. Flanagan, G. W. Brodland, and C. R. Ethier. Strain uniformity in biaxial specimens is highly sensitive to attachment details. *J. Biomech. Eng.* 131:091003, 2009.
- ¹⁸Feiner, B., J. Jelovsek, and C. Maher. Efficacy and safety of transvaginal mesh kits in the treatment of prolapse of the vaginal apex: a systematic review. *BJOG* 116:15–24, 2009.
- ¹⁹Fung, Y.-C. Elasticity of soft tissues in simple elongation. *Am. J. Physiol.* 213:1532–1544, 1967.
- ²⁰Fung, Y.-C. Biorheology of soft tissues. *Biorheology* 10:139–155, 1973.
- ²¹Fung, Y.-C. Biomechanics: Mechanical Properties of Living Tissues. New York: Springer, 1993.
- ²²Gabriel, B., D. Denschlag, H. Göbel, C. Fittkow, M. Werner, G. Gitsch, and D. Watermann. Uterosacral ligament in postmenopausal women with or without pelvic organ prolapse. *Int. Urogynecol. J.* 16:475–479, 2005.
- ²³Gabriel, B., D. Watermann, K. Hancke, G. Gitsch, M. Werner, C. Tempfer, and A. Zur Hausen. Increased expression of matrix metalloproteinase 2 in uterosacral ligaments is associated with pelvic organ prolapse. *Int. Urogynecol. J.* 17:478–482, 2006.
- ²⁴Gruber, D. D., W. B. Warner, E. D. Lombardini, C. M. Zahn, and J. L. Buller. Anatomical and histological examination of the porcine vagina and supportive structures: In search of an ideal model for pelvic floor disorder evaluation and management. *Female Pelvic Med. Reconstr. Surg.* 17:110–114, 2011.
- ²⁵Hingorani, R. V., P. P. Provenzano, R. S. Lakes, A. Escarcega, and R. Vanderby Jr. Nonlinear viscoelasticity in rabbit medial collateral ligament. *Ann. Biomed. Eng.* 32:306–312, 2004.
- ²⁶Iwanaga, R., D. J. Orlicky, J. Arnett, M. K. Guess, K. J. Hurt, and K. A. Connell. Comparative histology of mouse, rat, and human pelvic ligaments. *Int. Urogynecol. J.* 27:629–635, 2016.
- ²⁷Jacobs, N. T., D. H. Cortes, E. J. Vresilovic, and D. M. Elliott. Biaxial tension of fibrous tissue: using finite element methods to address experimental challenges arising from boundary conditions and anisotropy. *J. Biomech. Eng.* 135:021004, 2013.
- ²⁸Jelovsek, J. E. and M. D. Barber. Women seeking treatment for advanced pelvic organ prolapse have decreased body image and quality of life. *Am. J. Obstet. Gynecol.* 194:1455–1461, 2006.
- ²⁹Kielty, C. M., M. J. Sherratt, and C. A. Shuttleworth. Elastic fibres. *J. Cell. Sci.* 115:2817–2828, 2002.
- ³⁰Kobayashi, M., T. Takatori, K. Iwadata, and M. Nakajima. Reconsideration of the sequence of rigor mortis through postmortem changes in adenosine nucleotides and lactic acid in different rat muscles. *Forensic Sci. Int.* 82:243–253, 1996.
- ³¹Kobayashi, M., T. Takatori, M. Nakajima, K. Saka, H. Iwase, M. Nagao, H. Nijima, and Y. Matsuda. Does the sequence of onset of rigor mortis depend on the proportion of muscle fibre types and on intra-muscular glycogen content? *Int. J. Legal. Med.* 112:167–171, 1999.
- ³²Krompecher, T. Experimental evaluation of rigor mortis v. effect of various temperatures on the evolution of rigor mortis. *Forensic Sci. Int.* 17:19–26, 1981.
- ³³Lehr, H.-A., C. M. van der Loss, P. Teeling, and A. M. Gown. Complete chromogen separation and analysis in double immunohistochemical stains using photoshop-based image analysis. *J. Histochem. Cytochem.* 47:119–125, 1999.
- ³⁴Lionello, G., C. Sirieix, and M. Baleani. An effective procedure to create a speckle pattern on biological soft tissue for digital image correlation measurements. *J. Mech. Behav. Biomed.* 39:1–8, 2014.
- ³⁵Lowder, J. L., C. Ghetti, C. Nikolajski, S. S. Oliphant, and H. M. Zyczynski. Body image perceptions in women with pelvic organ prolapse: a qualitative study. *Am. J. Obstet. Gynecol.* 204:441–e1, 2011.
- ³⁶Luo, J., T. M. Smith, J. A. Ashton-Miller, and J. O. DeLancey. In vivo properties of uterine suspensory tissue in pelvic organ prolapse. *J. Biomech. Eng.* 136:021016, 2014.
- ³⁷Martins, P., A. L. Silva-Filho, A. M. Fonseca, A. Santos, L. Santos, T. Mascarenhas, R. M. Jorge, and A. M. Ferreira. Strength of round and uterosacral ligaments: A biomechanical study. *Arch. Gynecol. Obstet.* 287:313–318, 2013.
- ³⁸Ota, S., Y. Furuya, and K. Shintaku. Studies on rigor mortis. *Forensic Sci.* 2:207–219, 1973.
- ³⁹Pinto, J. and P. Patitucci. Visco-elasticity of passive cardiac muscle. *J. Biomech. Eng.* 102:57–61, 1980.
- ⁴⁰Ramanah, R., M. B. Berger, B. M. Parratte, and J. O. DeLancey. Anatomy and histology of apical support: a

- literature review concerning cardinal and uterosacral ligaments. *Int. Urogynecol. J.* 23:1483–1494, 2012.
- ⁴¹Reay Jones, N. H. J., J. C. Healy, L. J. King, S. Saini, S. Shousha, and T. G. Allen-Mersh. Pelvic connective tissue resilience decreases with vaginal delivery, menopause and uterine prolapse. *Br. J. Surg.* 90:466–472, 2003.
- ⁴²Riviaux, G., C. Rubod, B. Dedet, M. Brieu, B. Gabriel, and M. Cosson. Comparative analysis of pelvic ligaments: a biomechanics study. *Int. Urogynecol. J.* 24:135–139, 2013.
- ⁴³Smith, T. M., J. Luo, Y. Hsu, J. Ashton-Miller, and J. O. DeLancey. A novel technique to measure in vivo uterine suspensory ligament stiffness. *Am. J. Obstet. Gynecol.* 209:484.e1, 2013.
- ⁴⁴Sun, W., M. S. Sacks, and M. J. Scott. Effects of boundary conditions on the estimation of the planar biaxial mechanical properties of soft tissues. *J. Biomech. Eng.* 127:709–715, 2005.
- ⁴⁵Tan, T., N. M. Cholewa, S. W. Case, and R. De Vita. Micro-structural and biaxial creep properties of the swine uterosacral-cardinal ligament complex. *Ann. Biomed. Eng.* 44:3225–3237, 2016.
- ⁴⁶Tan, T., F. M. Davis, D. D. Gruber, J. C. Massengill, J. L. Robertson, and R. De Vita. Histo-mechanical properties of the swine cardinal and uterosacral ligaments. *J. Mech. Behav. Biomed.* 42:129–137, 2015.
- ⁴⁷Vardy, M. D., T. R. Gardner, F. Cosman, R. J. Scotti, M. S. Mikhail, A. O. Preiss-Bloom, J. K. Williams, J. M. Cline, and R. Lindsay. The effects of hormone replacement on the biomechanical properties of the uterosacral and round ligaments in the monkey model. *Am. J. Obstet. Gynecol.* 192:1741–1751, 2005.
- ⁴⁸Waldman, S., M. Sacks, and J. Lee. Boundary conditions during biaxial testing of planar connective tissues. Part II: Fiber orientation. *J. Mater. Sci. Lett.* 21:1215–1221, 2002.
- ⁴⁹Waldman, S. D. and J. M. Lee. Boundary conditions during biaxial testing of planar connective tissues. Part I: Dynamic behavior. *J. Mater. Sci. Mater. Med.* 13:933–938, 2002.
- ⁵⁰Woo, S. Mechanical properties of tendons and ligaments. I. Quasi-static and nonlinear viscoelastic properties. *Biorheology* 19:385, 1982.
- ⁵¹Wu, J. M., A. F. Hundley, R. G. Fulton, and E. R. Myers. Forecasting the prevalence of pelvic floor disorders in us women: 2010 to 2050. *Obstet. Gynecol.* 114:1278–1283, 2009.